Supporting Information

Belgardt et al. 10.1073/pnas.1001796107

SI Methods

Animal Care. Care of all animals was within institutional animal care committee guidelines. All animal procedures were conducted in compliance with protocols and approved by local government authorities (Bezirksregierung Köln, Cologne, Germany) and were in accordance with National Institutes of Health guidelines. Mice were housed in groups of 3–5 at 22–24 °C using a 12-h light/12-h dark cycle. Animals were fed either normal chow diet (Teklad Global Rodent 2018; Harlan) containing 53.5% carbohydrates, 18.5% protein, and 5.5% fat (12% of calories from fat) or a high-fat diet (HFD; C1057; Altromin) containing 32.7% carbohydrates, 20% protein, and 35.5% fat (55.2% of calories from fat). Animals had ad libitum access to water at all times, and food was only withdrawn if required for an experiment. Body weight was measured once a week; body length (naso-anal length) was measured before sacrifice. Genotyping was performed by PCR using genomic DNA isolated from tail tips. Primers to detect loxP flanked or WT JNK1 alleles were JNK1 no. 1, 5′-ACATGTACCATGT-ACTGACCTAAG-3′ and JNK1 no. 2, 5′-CATTACTCTA CTC-ACTATAG TAACA-3′. For detection of deletion, the primer set of JNK1 no.1 and JNK1Δ 5′-GATATCAGTA TATGTCCTTA TAG-3′ was used. Mice were killed using CO_2.

Lipid Analysis. Samples of mouse liver tissue (50–150 mg, $n = 4$) were homogenized with the Homogenizator Precellys 24 (Peqlab) in 1 mL of water at 6.500 rpm for 30 s. The protein content of the homogenate was routinely determined using bicinchoninic acid. After addition of 4 mL of methanol and 2 mL of chloroform, lipids were extracted for 24 h at 37 °C. The liquid phase was separated by filtration, and the insoluble tissue residues were further extracted for 24 h at 37 °C in 6 mL of methanol/chloroform 1:1 (vol/vol) and finally in 6 mL of methanol/chloroform 1:2 (vol/vol). The extracts were pooled, and the solvent was evaporated in a stream of nitrogen. The residues were purified using a modification of the Bligh-Dyer procedure as previously described (1). Lipids were applied to 20 × 10 cm high-performance TLC (HPTLC) Silica Gel 60 plates (Merck), which were prewashed twice with chloroform/methanol 1:1 (vol/vol) and air-dried for 30 min. For quantification of triacylglycerols and cholesteryl esters, each lane of the TLC plate was loaded with the equivalent of 50 μg and 1 mg wet weight of liver tissue, respectively. The TLC solvent system used was hexane/toluene 1:1 (vol/vol), followed by hexane/diethyl ether/glacial acetic acid 80:20:1 (vol/vol). For quantification of cholesterol, diacylglycerols, and free fatty acids, the equivalent of 2.5 mg of liver tissue was applied to 20 × 20 cm TLC plates, which were developed in hexane/diethyl ether/formic acid 30:50:1 (vol/vol/vol). For quantitative analytical TLC determination, increasing amounts of standard lipids (Sigma-Aldrich) were applied to the TLC plates in addition to the lipid samples. For detection of lipid bands, the TLC plates were sprayed with a phosphoric acid/copper sulfate reagent (15.6 g of $CuSO_4(H_2O)_5$ and 9.4 mL of H_3PO_4 (85%, wt/vol) in 100 mL of water) and charred at 180 °C for 10 min. Lipid bands were then quantified by densitometry using the TLC-Scanner 3 (CAMAG) at a wavelength of 595 nm.

Analysis of RNA Expression. mRNA expression was analyzed using quantitative RT-PCR. cDNA was isolated using RNeasy system (Qiagen) according to the manufacturer's instructions and amplified using TaqMan Universal PCR Master Mix, No AmpErase UNG with TaqMan Assay-on-Demand kits (Applied Biosystems), with the exception of GH (GH probe: GTTCGAGCGTGC- CT ACATTC; GH sense primer GCCCTTGTCCAGTCTGTTTTC, GH antisense primer GATGGTCTCTGAGAAGCAGAAAG) and JNK1 (JNK1 probe: AGTGTGTGCAG- CTTATGATGCC; JNK1 sense ATTGGAGATTCTACATTCACAGTCCTA, JNK1 antisense CATTCTGAAATGGCCGGCT). Relative expression of samples was adjusted for total RNA content by glucoronidase β expression. Calculations were performed by a comparative method (2-ddCt). Quantitative PCR was performed on an ABI Prism 7700 sequence detector (Applied Biosystems).

Generation of JNK1$^{fl/fl}$ and JNK1 $^{\Delta NES}$ Mice. We generated a JNK1 locus targeting vector in which exon 2 was flanked by loxP sites. This vector was transfected into F_1 ES cells, which were screened for correct integration by standard Southern blot methods. Correctly targeted ES cells were used to generate chimeras, which were backcrossed on a C57/bl6 background and examined for germline transmission. Afterward, JNK1$^{fl/wt}$ mice were backcrossed on a C57/bl6 background for three additional times before being intercrossed to generate JNK1$^{fl/fl}$ mice. JNK1$^{\Delta NES}$ mice were generated by crossing JNK1$^{fl/fl}$ mice with Nestin-Cre mice (which were on a pure C57BL/6 background). Male JNK1$^{\Delta NES}$ mice were bred with female JNK1$^{fl/fl}$ mice at all times. The background was unchanged throughout all experiments. Littermates were used for analysis at all times.

Analytical Procedures. Blood glucose values were determined from whole venous blood using an automatic glucose monitor (GlucoMen; A. Menarini Diagnostics). Serum hormones were measured by ELISA using mouse standards according to the manufacturer's guidelines (mouse leptin ELISA, no. 90030, Crystal Chem; rat/mouse insulin ELISA, no. INSKR020, Crystal Chem; mouse growth hormone ELISA, no. EZRMGH-45K, Millipore; and mouse IGF1 ELISA, no. MG100, R&D Systems). Brain areas of interest (arcuate nucleus and hypothalamus) were dissected with the aid of a mouse brain atlas using a coronal acrylic brain matrix (Braintree Scientific).

EMSA. EMSA was performed using standard protocols with AP1 (sc-2501) and SP1 (sc-2502) oligomers (Santa Cruz) (2).

Indirect Calorimetry, Physical Activity, and Food Intake. All measurements were performed in a PhenoMaster system (TSE Systems), which allows measurement of metabolic performance and activity monitoring by an infrared light-beam frame. Mice were placed at room temperature (22 °C–24 °C) in 7.1-l chambers of the PhenoMaster open circuit calorimetry. Mice were allowed to adapt to the chambers for at least 24 h. Food and water were provided ad libitum in the appropriate devices and measured by the build-in automated instruments. Locomotor activity and parameters of indirect calorimetry were measured for at least the following 48 h. Presented data are average values obtained in these recordings.

1. Signorelli P, Hannun YA (2002) Analysis and quantitation of ceramide. *Methods Enzymol* 345:275–294.

2. Ernst MB, et al. (2009) Enhanced Stat3 activation in POMC neurons provokes negative feedback inhibition of leptin and insulin signaling in obesity. *J Neurosci* 29:11582–11593.

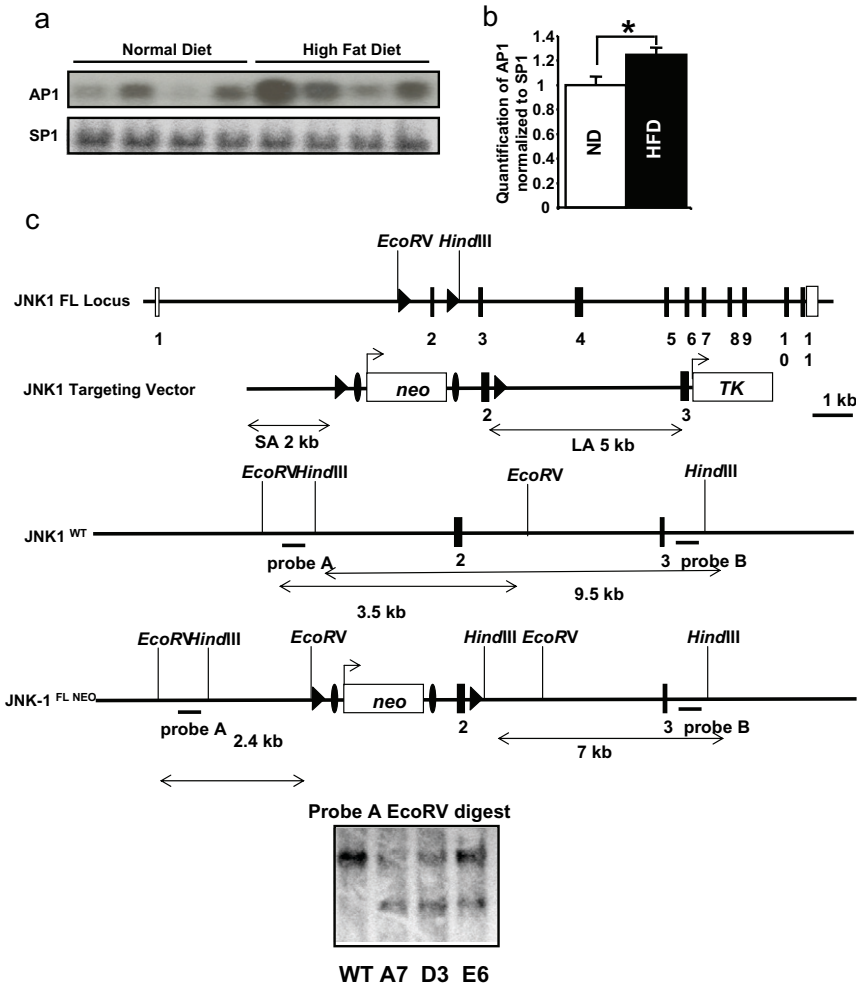

Fig. S1. Generation of mice with conditional JNK1 allele. (*A*) DNA-binding activity of JNK activated AP-1 and a nonregulated loading control (SP-1) was measured using electrophoretic mobility shift assay (EMSA) in arcuate nucleus extracts from normal diet (ND) and high-fat diet (HFD) fed C57BL/6 mice. (*B*) Quantification of the EMSA shown in Fig. 1*A*. AP-1 binding was normalized to SP-1 binding activity. *, $P \leq 0.05$. (*C*) Generation of the conditional JNK-1 allele. The JNK-1 targeting vector was created to flank exon 2 of the JNK1 gene by loxP sites. V6.5 ES cells were transfected and subsequently selected with G418 and Ganciclovir, respectively. Southern blot analysis of genomic DNA isolated from individual ES cell clones revealed correctly targeted clones A7, D3, and E6 using EcoRV-digested DNA transferred to a nylon membrane with the external probe A. In these clones, a 2.4-kb targeted band appeared in addition to the 3.5-kb WT band. ES cells were injected into blastocyst to generate JNK1 FL-neo mice. These were further intercrossed with Flp deleter mice to excise the neo cassette by Flp-mediated recombination.

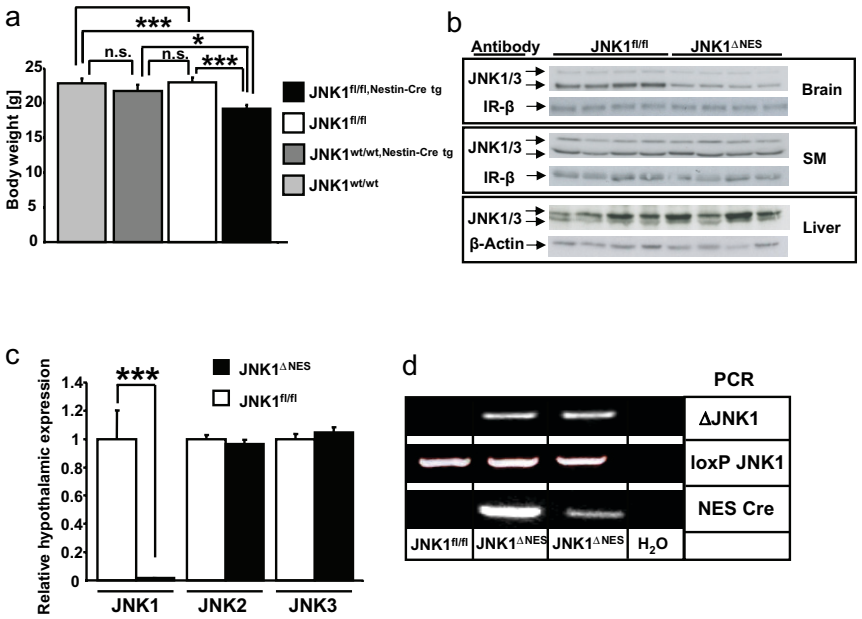

Fig. S2. Specificity of JNK1 ablation in JNK1$^{\Delta NES}$ mice. (*A*) Presence of Nestin-Cre construct or loxP flanked JNK1 allele does not impair body weight control. Body weight of wild type, Nestin-Cre transgenic, control, and JNK1$^{\Delta NES}$ mice at the age of 6 weeks is shown. *, $P \leq 0.05$; ***, $P \leq 0.001$. (*B*) Western blot analysis of JNK1/3 and IR-β or β-actin expression (loading control) in whole brain, liver, and skeletal muscle (SM) of JNK1$^{\Delta NES}$ and JNK1$^{fl/fl}$ mice ($n = 4$ per group). (*C*) Hypothalamic expression of JNK 1, 2, and 3 in JNK1$^{fl/fl}$ (□) and JNK1$^{\Delta NES}$ (■)mice ($n = 6$ per group) as measured by real-time–PCR. ***, $P \leq 0.001$. (*D*) Deletion of the JNK1 allele in the pituitary of JNK1$^{\Delta NES}$ mice. After DNA extraction from the pituitary, PCR was used to detect the deleted JNK1 allele (ΔJNK1), the loxp-flanked JNK1 alleles, as well as presence of the Nestin-Cre transgene.

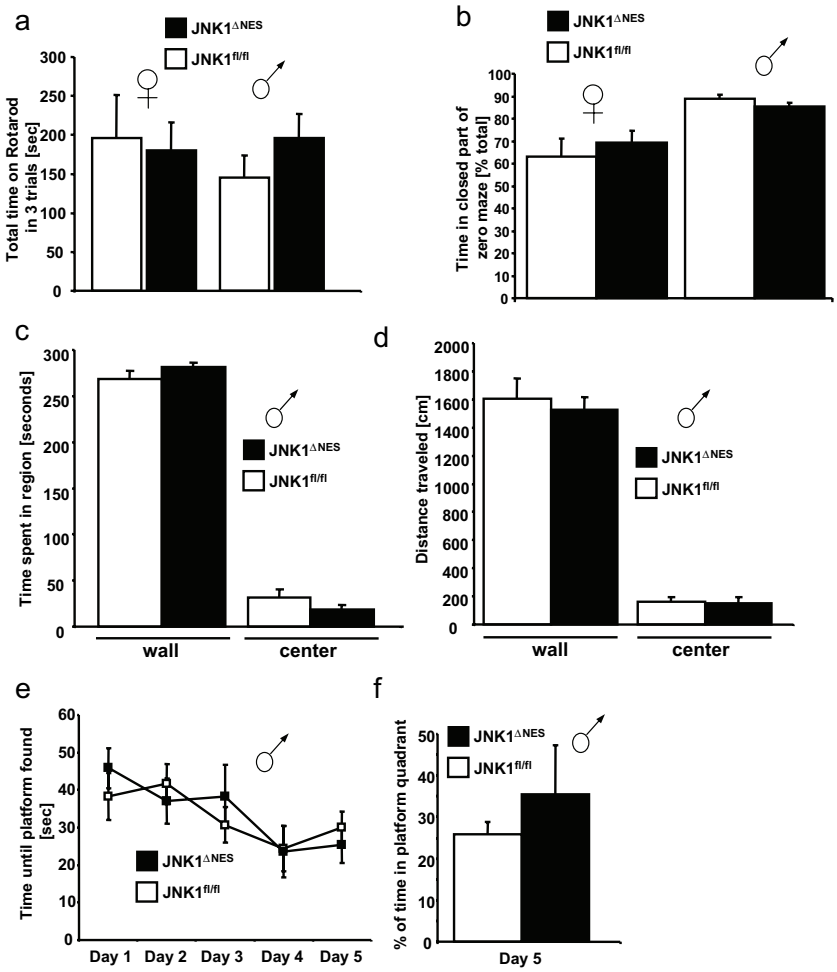

Fig. S3. Behavioral analysis of JNK1$^{\Delta NES}$ mice. (*A*) Rotarod analysis of control and JNK1$^{\Delta NES}$ mice. Control and JNK1$^{\Delta NES}$ mice were mounted on the Rotarod, and total time on the rotating rod until mouse fell from the rotarod was measured (n = 8 per genotype and sex). (*B*) Zero maze analysis of control and JNK1$^{\Delta NES}$ mice. Control and JNK1$^{\Delta NES}$ mice were put on the zero maze, and the time in which the mouse stayed in the closed part of the maze was tracked by an automatic visual system (n = 8 per genotype and sex). (*C*) Open field analysis of control and JNK1$^{\Delta NES}$ mice. Control and JNK1$^{\Delta NES}$ mice were put into the open field, and the time in which the mouse stayed close to the wall was tracked by an automatic computer-based system (n = 8 per genotype). (*D*) Open field analysis of control and JNK1$^{\Delta NES}$ mice. Control and JNK1$^{\Delta NES}$ mice were put into the open field, and the distance the mouse traveled close to the wall was tracked by an automatic computer-based system (n = 8 per genotype). (*E*) Morris water maze analysis of control and JNK1$^{\Delta NES}$ mice. Control and JNK1$^{\Delta NES}$ mice were trained daily for 4 days to memorize the location of the platform, and the time taken by each mouse to find the platform was measured by an automatic, software-based system (n = 8 per genotype). (*F*) On the fifth day of the Morris water maze analysis, the platform was removed from the pool, and the time the mouse swam in the quadrant in which the platform had been was automatically measured by an automatic, software-based system (n = 8 per genotype).

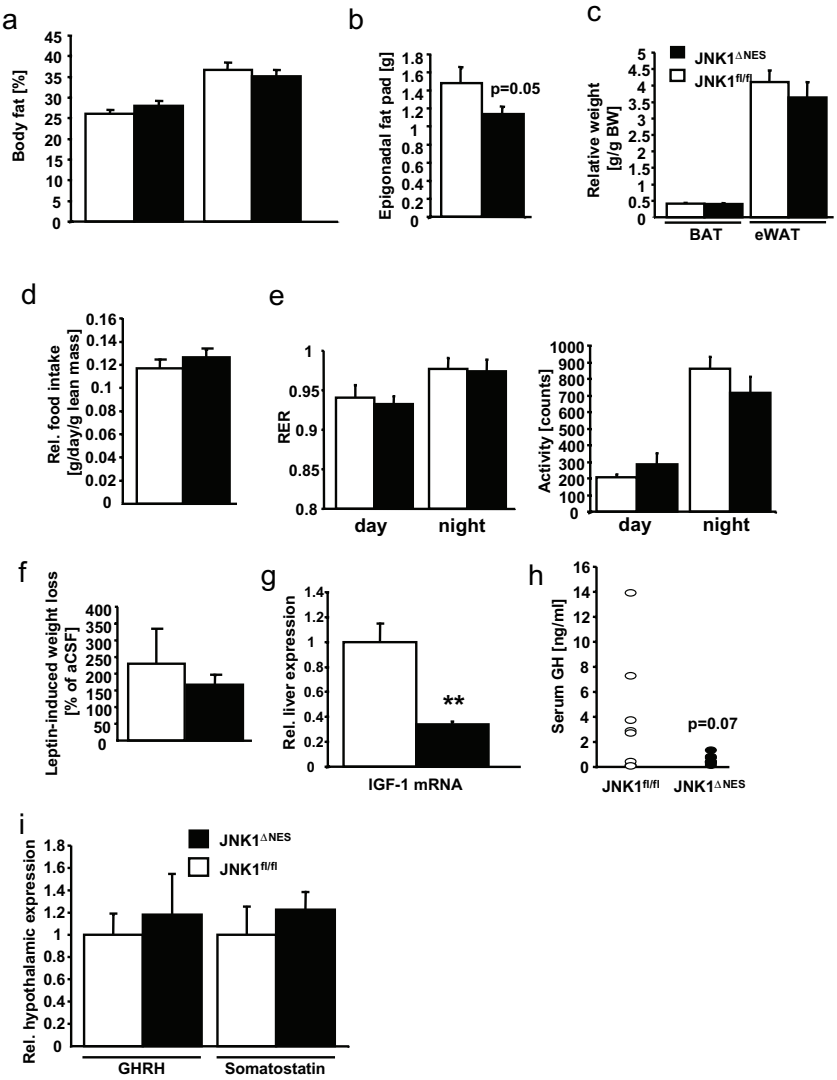

Fig. S4. Additional phenotyping of JNK1$^{\Delta NES}$ mice. (*A*) Body fat content of JNK1$^{fl/fl}$ (□) and JNK1$^{\Delta NES}$ (■) mice on ND and HFD at the age of 16 weeks as measured by NMR analysis (n = 12 per group). (*B*) Absolute epigonadal adipose tissue mass of control and JNK1$^{\Delta NES}$ mice on normal diet at the age of 16 weeks (n = 9 per group). (*C*) Relative white and brown adipose tissue weight of JNK1$^{fl/fl}$ (□) and JNK1$^{\Delta NES}$ (■) mice on normal diet at the age of 16 weeks (n = 12 per group). Relation of epigonadal adipose mass and brown adipose tissue mass to body weight was calculated individually for each mouse. (*D*) Relative food intake of JNK1$^{fl/fl}$ (□) and JNK1$^{\Delta NES}$ (■) mice on normal diet at the age of 13 weeks (n = 8 per group). Relation of food intake to body weight was calculated individually for each mouse. (*E*) Daily and nightly respiratory quotient (RER) and activity of control and JNK1$^{\Delta NES}$ mice on normal diet at the age of 13 weeks (n = 8 per group). (*F*) Body weight loss 24 h after intracerebroventricular leptin treatment in JNK1$^{fl/fl}$ (□) (n = 5) and JNK1$^{\Delta NES}$ (■) mice (n = 4) mice on normal diet at the age of 12 weeks. Mice were injected with either vehicle or 2 μg leptin immediately before onset of dark phase, and body weight was measured 24 h later. Shown is fold change of body weight after leptin injection compared to vehicle injection. (*G*) Hepatic IGF1 mRNA expression as measured by real-time–PCR (n = 7 per group). (*H*) Serum GH concentrations of JNK1$^{fl/fl}$ (□) (n = 8) and JNK1$^{\Delta NES}$ (■) (n = 8) on normal diet at the age of 10 weeks. (*I*) Hypothalamic expression of GHRH and somatostatin of JNK1$^{fl/fl}$ (□) (n = 6) and JNK1$^{\Delta NES}$ (■) (n = 6) mice on normal diet at the age of 16 weeks as measured by real-time–PCR.

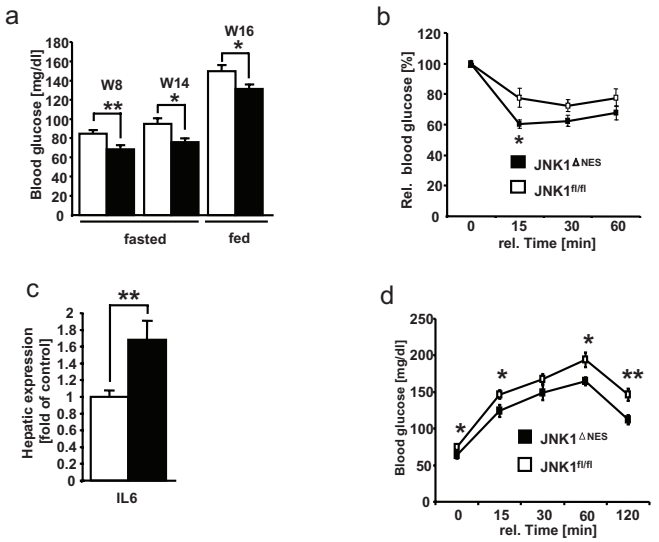

Fig. S5. Additional analysis of glucose homeostasis of JNK1$^{\Delta NES}$ mice. (*A*) Fasted and fed blood glucose concentration of JNK1$^{fl/fl}$ (□) and JNK1$^{\Delta NES}$ (■) mice on high-fat diet at the indicated ages (n = 10–17 per group). (*B*) Intraperitoneal glucose tolerance test in JNK1$^{fl/fl}$ and JNK1$^{\Delta NES}$ mice on normal diet at the age of 14 weeks (n = 10 per group). *, $P \leq 0.05$. (*C*) Real-time analysis of hepatic interleukin 6 (IL6) mRNA expression in JNK1$^{fl/fl}$ and JNK1$^{\Delta NES}$ mice on high-fat diet at the age of 16 weeks (n = 8 per group). **, $P \leq 0.01$. (*D*) Pyruvate tolerance test in JNK1$^{fl/fl}$ (□) and JNK1$^{\Delta NES}$ (■) mice on high-fat diet at the age of 10 weeks (n = 8–14 per group).

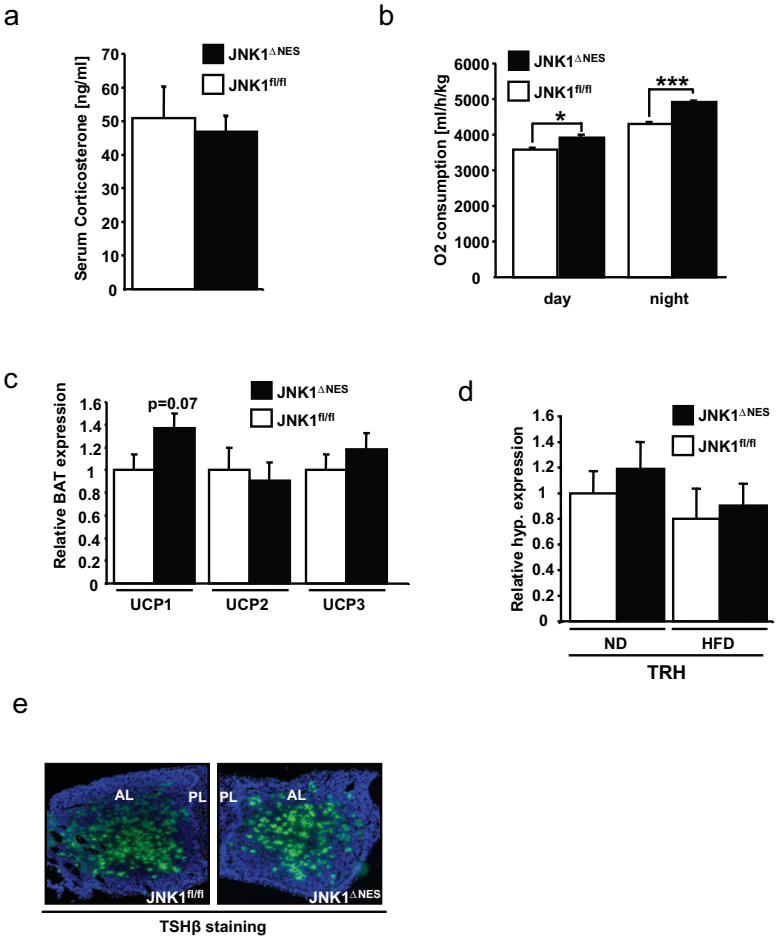

Fig. S6. Additonal pituitary analysis of $^{\Delta NES}$ mice. (*A*) Unchanged circulating corticosterone in JNK1$^{\Delta NES}$ mice. Serum corticosterone in control and JNK1$^{\Delta NES}$ mice at the age of 10 weeks was measured by ELISA. (n = 8 per genotype). (*B*) Daily and nightly oxygen consumption of JNK1$^{fl/fl}$ and JNK1$^{\Delta NES}$ mice on high-fat diet at the age of 13 weeks (n = 8 per group). Oxygen consumption was calculated per gram lean mass of each individual mouse. (*C*) Brown adipose tissue expression of UCP1, 2, and 3 of JNK1$^{fl/fl}$ (□) (n = 6) and JNK1$^{\Delta NES}$ (■) mice (n = 6) on high-fat diet at the age of 16 weeks as measured by real-time PCR. (*D*) Hypothalamic expression of TRH as measured by real-time analysis (n = 5 per genotype and diet).

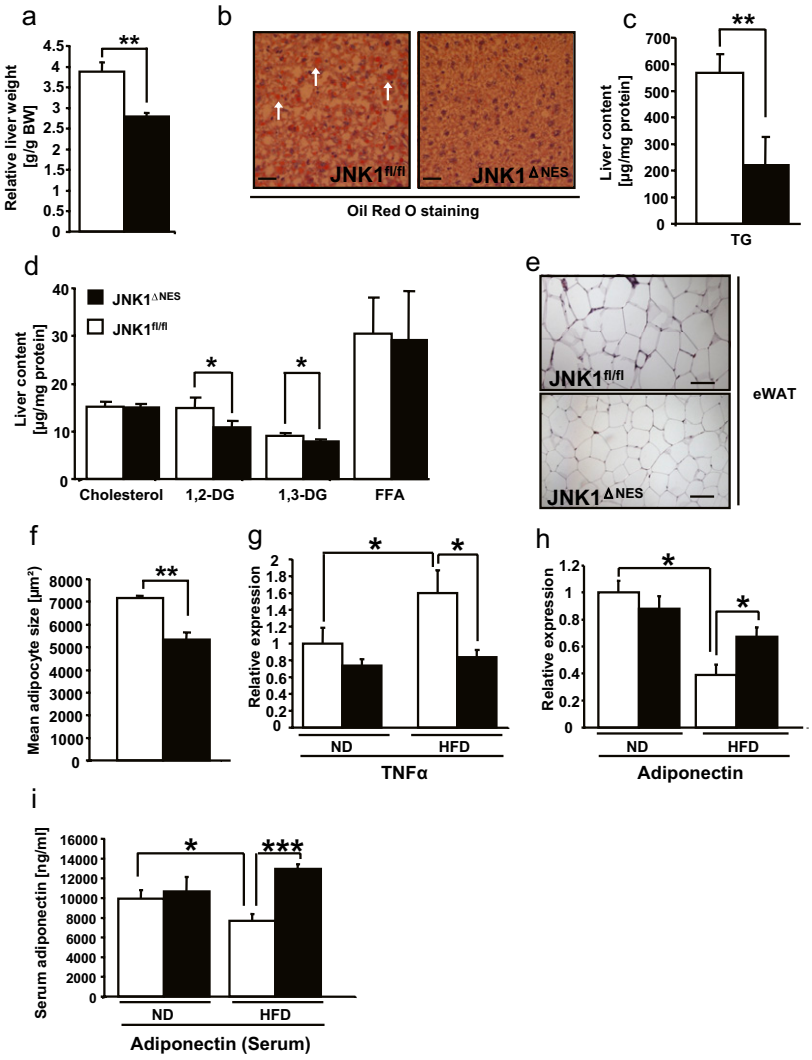

Fig. S7. Amelioration of obesity-induced hepatic and adipose dysfunction in JNK1$^{\Delta NES}$ mice. (*A*) Relative liver weight of JNK1$^{fl/fl}$ (□) and JNK1$^{\Delta NES}$ (■) mice on high-fat diet at the age of 16 weeks (n = 12 per group). Relation of liver mass to body weight was calculated individually for each mouse. (*B*) Representative oil red O staining of hepatic tissue of JNK1$^{fl/fl}$ and JNK1$^{\Delta NES}$ mice on high-fat diet at the age of 16 weeks (Original magnification, ×100.) (Scale bar, 40 μm.) Liver sections of 3 animals per genotype were analyzed. (*C*) Hepatic triglyceride (TG) content of JNK1$^{fl/fl}$ (□) and JNK1$^{\Delta NES}$ (■) mice on high-fat diet at the age of 16 weeks (n = 4 per group). (*D*) Hepatic cholesterol, 1,2- and 1,3-diacylglycerides (DG), and free fatty acid (FFA) content of JNK1$^{fl/fl}$ (□) and JNK1$^{\Delta NES}$ (■) mice on high-fat diet at the age of 16 weeks (n = 4 per group). (*E*) Representative H&E stain of epigonadal adipose tissue of control and JNK1$^{\Delta NES}$ mice on high-fat diet at the age of 16 weeks. (Scale bar, 100 μm.) (*F*) Quantification of adipocyte surface in epigonadal adipose tissue of JNK1$^{fl/fl}$ (□) and JNK1$^{\Delta NES}$ (■) mice on high-fat diet at the age of 16 weeks (n = 3–6 per group). (*G*) Real-time analysis of TNFα expression in epigonadal adipose tissue of JNK1$^{fl/fl}$ (□) and JNK1$^{\Delta NES}$ (■) mice on normal and high-fat diet at the age of 16 weeks (n = 8 per group). (*H*) Real-time analysis of adiponectin expression in epigonadal adipose tissue of JNK1$^{fl/fl}$ (□) and JNK1$^{\Delta NES}$ (■) mice on normal and high-fat diet at the age of 16 weeks (n = 8 per group). (*I*) Serum Adiponectin concentrations in JNK1$^{fl/fl}$ (□) and JNK1$^{\Delta NES}$ (■) mice on normal and high-fat diet at the age of 16 weeks (n = 6–12 per group).